Cell

A Saturated FG-Repeat Hydrogel Can Reproduce the Permeability Properties of Nuclear Pore Complexes

Steffen Frey[1] and Dirk Görlich[1,*]
[1] Max-Planck-Institut für Biophysikalische Chemie, Am Fassberg 11, D-37077 Göttingen and Zentrum für Molekulare Biologie der Universität Heidelberg (ZMBH), INF 282, D-69120 Heidelberg, Germany
*Correspondence: goerlich@mpibpc.mpg.de
DOI 10.1016/j.cell.2007.06.024

SUMMARY

The permeability barrier of nuclear pore complexes (NPCs) controls the exchange between nucleus and cytoplasm. It suppresses the flux of inert macromolecules $\geq$ 30 kDa but allows rapid passage of even very large cargoes, provided these are bound to appropriate nuclear transport receptors. We show here that a saturated hydrogel formed by a single nucleoporin FG-repeat domain is sufficient to reproduce the permeability properties of NPCs. Importin β and related nuclear transport receptors entered such hydrogel >1000× faster than a similarly sized inert macromolecule. The FG-hydrogel even reproduced import signal-dependent and importin-mediated cargo influx, allowing importin β to accelerate the gel entry of a large cognate cargo more than 20,000-fold. Intragel diffusion of the importin β-cargo complex occurred rapidly enough to traverse an NPC within ≈12 ms. We extend the "selective phase model" to explain these effects.

INTRODUCTION

Cell nuclei lack protein synthesis and therefore import all their proteins from the cytoplasm. In return, they supply the cytoplasmic compartment with nuclear products such as ribosomes, tRNAs, and mRNAs. The nuclear envelope (NE) encloses the nuclei and confines all nucleo-cytoplasmic exchange to nuclear pore complexes (NPCs), whose giant aqueous channels connect nucleoplasm and cytoplasm (reviewed in Suntharalingam and Wente, 2003). The permeability barrier of NPCs controls this exchange (reviewed in Burke, 2006; Elbaum, 2006). It is freely permeable for small molecules but suppresses the flux of inert macromolecules $\geq$ 30 kDa and thereby prevents an uncontrolled intermixing between nuclear and cytoplasmic contents.

Nuclear transport receptors (NTRs) catalyze NPC passage of objects that exceed this size limit: NTRs circulate rapidly between nucleus and cytoplasm and transfer recognized cargoes from one side of the NE to the other (reviewed in Görlich and Kutay, 1999; Pemberton and Paschal, 2005; Weis, 2002). The actual NPC passage of cargo-NTR complexes is reversible. It is therefore the active cargo release in the destination compartment that allows these NTRs to act as cargo pumps. In the case of importin β-type NTRs, switching in affinity for cargo is driven by the RanGTPase-system (reviewed in Görlich and Kutay, 1999).

NPCs are built from multiple copies of ≈30 different nucleoporins (Cronshaw et al., 2002; Rout et al., 2000). These nucleoporins not only form the rigid NPC scaffold, but many of them also contain so-called FG-repeat domains, which are crucial for the phenomenon of NTRs crossing the permeability barrier 100- to 1000-fold faster than inert molecules of the same size.

FG-repeat domains account for ≈12%–20% of the mass of an NPC (Rout et al., 2000; Rout and Wente, 1994) and fulfill redundant, but essential, functions (Strawn et al., 2004). They appear intrinsically unfolded (Denning et al., 2003) and comprise up to 50 FG-repeat units, in which a short cluster of hydrophobic residues is surrounded by a more hydrophilic spacer sequence (Denning and Rexach, 2006). FG repeats occur in various flavors, examples being FxFG repeats, where two phenylalanines (F) constitute a hydrophobic cluster, or GLFG repeats with F and leucine (L) as hydrophobic residues (Cushman et al., 2006; Denning and Rexach, 2006). NTRs bind these hydrophobic clusters and this binding is essential for facilitated NPC-passage of cargo-NTR complexes (Bayliss et al., 2002, 2000, 1999; Bednenko et al., 2003; Cushman et al., 2006; Frey et al., 2006; Fribourg et al., 2001; Ribbeck and Görlich, 2002). It is therefore reasonable to assume, although so far unproven, that FG repeats form, or at least contribute to, the permeability barrier of NPCs (discussed in Ribbeck and Görlich, 2001, 2002).

How a nucleoporin-NTR interaction accelerates NPC-passage is, however, not a trivial problem. In fact,

a mere binding should have the opposite effect and cause only a delay of NPC-passage.

To resolve this paradox, we previously proposed the "selective phase model" (Ribbeck and Görlich, 2001, 2002). The model assumes that interactions between the hydrophobic clusters crosslink the FG-repeat domains into a sieve-like FG-hydrogel, the "selective phase." The mesh size of the sieve sets the ≈30 kDa size-limit for unhindered NPC-passage of inert material. NTRs and their cargo-complexes typically exceed this size-limit and yet rapidly cross the barrier. We therefore proposed that NTRs catalyze their own barrier-passage, because hydrophobic clusters disengage from inter-repeat contacts upon NTR-binding. This way, NTRs could transiently open obstructing meshes and clear their way to the other side of the barrier. Since the hydrogel can re-seal behind the NTR, it would remain a firm barrier toward inert objects, even when very large cargo-NTR complexes transit the central NPC-channel.

We reported recently that hydrophobic and/or aromatic (π-π) interactions between the phenyl groups crosslink FG-repeat domains into the predicted elastic hydrogel (Frey et al., 2006). Furthermore, we provided evidence that such hydrogel-formation is essential for viability in yeast. We show now that a sufficiently concentrated FG-hydrogel possesses indeed very similar permeability-properties as NPCs. It excludes inert proteins, but allows rapid entry of importins and their cargo-complexes. Our data further suggest that NTRs not only bind the hydrophobic clusters of FG repeats, but also accelerate the dissociation of adjacent inter-repeat contacts by many orders of magnitude. We extend the selective phase model to accommodate these findings.

RESULTS

An Undersaturated FG-Hydrogel Is Only a Poor Barrier

The current key question for understanding NPC function is whether the permeability barrier of NPCs is indeed made of an FG-repeat hydrogel. If so, then such hydrogel should behave like the permeability barrier and exclude large inert molecules but allow rapid entry (and passage) of NTRs.

We decided to test this initially for one pair of permeation probes, namely the 124 kDa fusion between GFP and yeast importin β (Kap95p) serving as a representative of NTRs (Chi et al., 1995; Enenkel et al., 1995; Görlich et al., 1995; Iovine et al., 1995) and a 117 kDa derivative of the tetrameric Red fluorescent protein ("acRedStar") serving as our inert permeation probe. To make the latter more alike to the highly negatively charged GFP-importin β fusion, we had introduced 28 additional acidic residues into the acRedStar tetramer.

As a control, we first compared the entry of these two proteins into a matrix with inert pores (that interact with none of the probes). For that, we performed gel permeation chromatography (Figure S1) and observed that acRedStar entered the pores of a Superdex 200 matrix with an apparent Stokes radius (R_S) of 3.9 nm, slightly faster than GFP-importin β (R_S = 4.5 nm).

As an FG-repeat domain, we chose the N-terminal repeat domain from the yeast nucleoporin Nsp1p (Hurt, 1988); it contains regular FSFG and less regular FG repeats and will therefore be referred to as the fsFG domain. We prepared a hydrogel containing ≈0.27 mM of the fsFG domain (corresponding to 4.9 mM FxFG and 4.1 mM other FG repeats), mounted the gel onto the stage of a confocal laser-scanning microscope (Figure S2), and followed the influx of our inert permeation probe. acRedStar permeated rapidly into this hydrogel and diffused inside the gel nearly as fast as free in solution (Figures 1A–1C; Table 1). Only at the buffer-gel boundary did a slight delay become evident as a small step within the concentration profile across the buffer-gel boundary (Figure 1C; see Figure S5 for computer simulation of entry kinetics and discussion of curve shapes).

This rapid influx was initially quite unexpected because the meshes of a homogeneous hydrogel should allow a free passage of only those objects that have a smaller diameter ($2 \times R_S$) than the spacer length; in the case of the Nsp1-derived fsFG repeats, the Stokes radius of the diffusing species should be $\leq$ 2 nm (see Experimental Procedures and below). acRedStar (R_S = 3.9 nm) clearly exceeds this limit, and this raised the question of why it permeated into the gel so efficiently.

The Concept of a Saturated FG-Hydrogel

A pairwise interaction of all hydrophobic clusters within a homogeneous FG-hydrogel can occur only when the concentration of repeat units equals or exceeds a critical concentration, the "saturation limit." The right panel of Figure 1D depicts the simplest geometry of such saturated gel. Here, pairs of hydrophobic clusters are arranged as a cubic grid with unit length u, which requires two clusters per cube volume u^3. With N_A being Avogadro's number ($\approx 6 \times 10^{23}$ molecules per mole), the cluster concentration is then given by:

$$c_{repeats} = \frac{2}{u^3 \cdot N_A} \quad (1)$$

The unit length equals the mean distance between two adjacent hydrophobic clusters on the linear polymer. For the regular (19 residues long) FSFG repeats from Nsp1p, we estimated a unit length of $u \approx 4$ nm (see Experimental Procedures) and hence a saturation limit of ≈50 mM repeat units. This is a ≈6- to 10-fold higher concentration than in the FG-hydrogel from Figures 1A–1C (depending on whether only regular FSFG-repeat units or all FG repeats of the fsFG domain are counted).

Since the minimal distance between two adjacent hydrophobic clusters cannot increase beyond the length of the connecting polypeptide backbone, a lower density gel cannot be formed by "stretching the grid" of a saturated gel. Instead, interrepeat contacts must be abandoned and

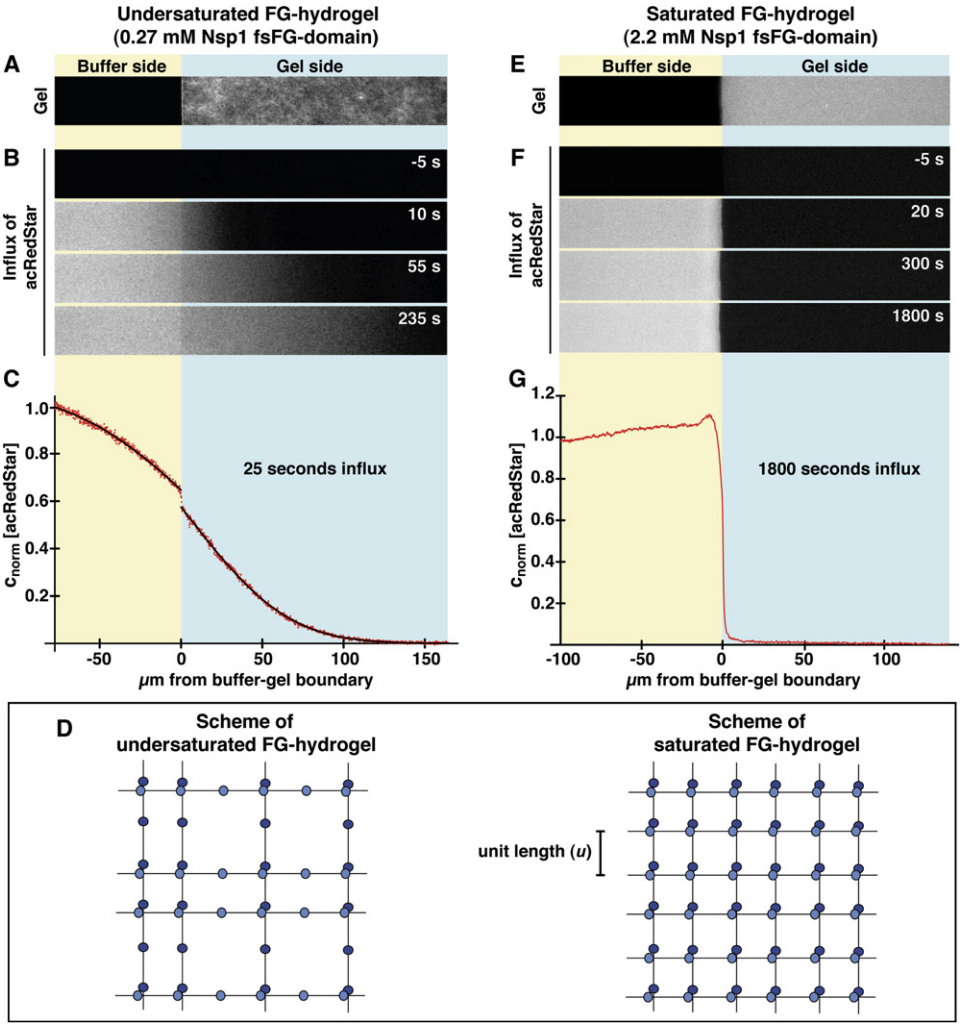

Figure 1. Only a Saturated FG-Hydrogel Poses a Firm Barrier against Influx of acRedStar

(A) A hydrogel containing 0.27 mM unlabelled and 1 μM Alexa 633-labeled Nsp1 fsFG-repeat domain was prepared, mounted to the stage of a confocal laser scanning microscope, and imaged after excitation at 633 nm.

(B) Panels show influx of the 117 kDa acRedStar protein into the hydrogel from (A). acRedStar entered the gel rapidly (entry rate ≈5 μm/s).

(C) Red points show profile of acRedStar concentration through the buffer-gel boundary at the 25 s time point. A slight delay in gel entry is indicated by the small concentration step at the buffer-hydrogel interphase. The black curve represents fits to error functions (see Experimental Procedures), from which diffusion constants in buffer and within the gel were derived. The data indicate that acRedStar diffused inside this low-concentrated FG-hydrogel not significantly slower than free in solution. See Figure S5 for computer simulations.

(D) Right: Cartoon of a saturated FG-hydrogel, where all hydrophobic clusters have engaged into pairwise contacts. The simplest geometry with an orthogonal grid is shown. Since the maximal distance between adjacent clusters (u) is limited by the spacer length, such arrangement requires that the concentration of repeat units exceeds a certain threshold, the "saturation limit." For details, see main text. Left: Cartoon depicts a gel with a lower concentration of repeat units than the saturation limit. Some hydrophobic clusters fail to find a sufficiently close partner for forming an interrepeat contact. Compared to saturated hydrogels, larger meshes result. The scheme depicts an "undersaturated" gel with defects of minimal size. Alternatively, such small defects could fuse to a larger one. This would make the gel less homogeneous (as observed for the low-concentrated gel in [A]) but would allow more hydrophobic clusters to engage into mutual contacts.

(E) A hydrogel containing 2.2 mM of Nsp1 fsFG-repeat domain was formed and visualized as in (A).

(F) Frames show influx of acRedStar into the hydrogel from (E). Only very small amounts entered the gel, even after a >7-fold longer incubation time as compared to the experiment shown in (A)–(C).

(G) Red curve shows profile of acRedStar concentration at the 1800 s time point. Quantitation and fitting the data of all time points to diffusion models indicate that the influx of acRedStar into this saturated FG-hydrogel ($k_f \approx 1$ nm/s) proceeded ≈5000-fold more slowly than into the undersaturated FG-hydrogel from (A)–(C).

Table 1. Summary of Entry Kinetics of Indicated Mobile Species into an Undersaturated or Saturated FG-Hydrogel

Barrier	Mobile Species	Mass (kDa)	Entry Rate into Barrier (μm/s)	Partition Coefficient (gel:buffer)	Intrabarrier Diffusion Constant ($\mu m^2/s$)	Flux through a Barrier-Filled Pore at $\Delta c = 1$ μM (molecules/s)
Water (Calculated)	acRedStar	117	n.a.	1	60	1000
FG-Hydrogel 0.27 mM fsFG-Repeat Domain	acRedStar	117	5	~1	40–50	3
FG-Hydrogel 2.2 mM fsFG-Repeat Domain	acRedStar	117	0.001–0.01	0.1–1	0.2–1	0.0006–0.006
	GFP-importin β (Kap95p)	124	>10–20[a]	>100[a]	0.1–0.2	>6–12[a]
	GFP-Pse1p (Kap121p)	151	>35[a]	>300[a]	0.05–0.1	>20[a]
	GFP-Pdr6p (Kap122p)	153	>20[a]	>300[a]	0.05–0.1	>12[a]
	GFP-Yrb4p (Kap123p)	152	>7[a]	>150[a]	0.05–0.1	>4[a]
	transportin	102	>25[a]	>800[a]	0.03–0.1	>15[a]
	acGFP	28	0.5	n.d.	n.d.	0.3
	Ntf2p	30	>13[a]	>100[a]	0.1–0.5	>8[a]
	IBB-RedStar	150	0.001–0.01	0.1–1	0.2	0.0005–0.005
	IBB-RedStar + importin β	530	>50[a]	>1000[a]	0.1	>30[a]

For experimental details see Figures 1–3, 5, and S3. For details of parameter estimation see Experimental Procedures. For computer simulation and discussion of entry kinetics, see also Figure S5. For estimating fluxes through vertebrate NPC-sized channels, we applied Equation 2 (Figure S4), set diameter and length of the pore to each 50 nm, and assumed for the mobile species 1 μM concentration difference across the pore.

[a] Entry rates can here be given only as lower limits because the true depth of the depletion zone in front of the gel is obscured by the very bright signal within the barrier. For the same reason and because the massive fluxes into the gel prevented reaching the equilibrium concentrations at the buffer-gel boundaries, partition coefficients are also only lower estimates.

larger meshes must form in undersaturated gels (Figure 1D, left panel). Such larger meshes would plausibly explain why the undersaturated FG-hydrogel from Figures 1A–1C performed so poorly as a barrier.

Permeability Properties of a Saturated FG-Hydrogel Resemble Those of NPCs

After optimizing the gelling procedure, we were able to prepare FG-hydrogels that were denser than the saturation limit and that contained up to 2.2 mM of the fsFG-repeat domain (corresponding to 39 mM FSFG and 32 mM other FG repeats). Such gels not only had a far greater mechanical strength (data not shown), but were also more homogeneous than the low-density gels (compare Figures 1A and 1E). The most striking effect was, however, that the saturated FG-hydrogel became an efficient barrier that firmly excluded the acRedStar protein. Compared to the 0.27 mM fsFG-repeat domain gel, the influx rate dropped 500- to 5000-fold. Compared to a water-water boundary (calculated as a 50 nm thick water layer), influx was even 10^5- to 10^6-fold slower (Figures 1E–1G, S3, and S5; Table 1). Also, intragel diffusion became reduced at least 50-fold compared to diffusion in buffer.

We then studied the GFP-importin β-fusion and observed a strikingly different interaction with the FG-hydrogel (Figures 2 and S3). This NTR rapidly dissolved within the gel, reaching a partition coefficient of >100. The FG-hydrogel thus behaved as previously predicted by the selective phase model, i.e., it constituted an excellent solvent for importin β (Ribbeck and Görlich, 2001, 2002). Importin β was indeed absorbed so efficiently that a deep depletion zone formed in front of the gel, where the concentration of importin β dropped to <1%–10% of the free concentration in buffer. Note that the depth of the depletion zone is probably still underestimated because it had to be imaged against the very bright signal in the hydrogel. The FG-hydrogel thus behaved like a "perfect sink" for NTRs, i.e., diffusion of importin β to the gel surface was rate limiting and not its actual entry into the gel. From the time course of absorption and the

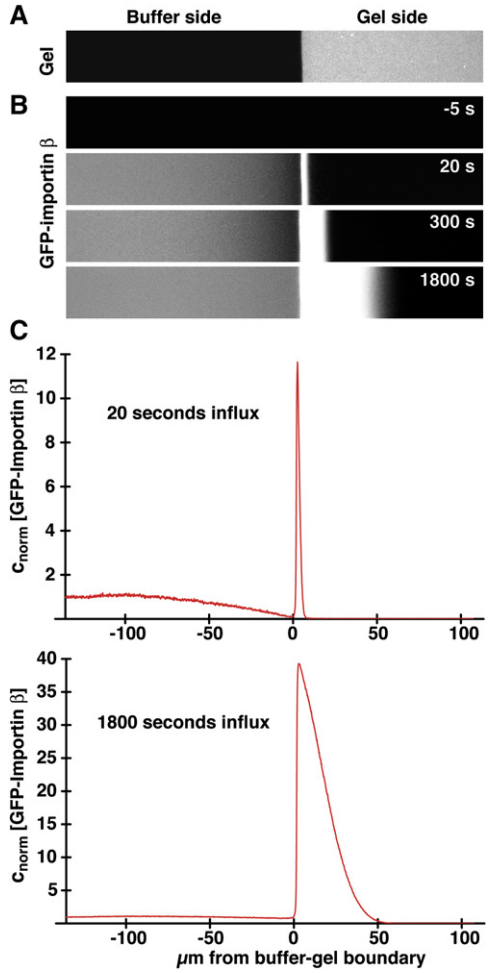

Figure 2. GFP-Importin β Rapidly Enters the Saturated FG-Hydrogel

(A) Image of the saturated FG-hydrogel used for this experiment (same batch as in Figures 1E–1G).

(B) Frames show at indicated time points the influx of GFP-importin β into the hydrogel. To visualize the mobile species also in the buffer side, the gel side of the frames had to be overexposed.

(C) Profiles of GFP-importin β concentration at indicated time points, normalized to the free concentration in the buffer. Note the deep depletion zone in front of the barrier, best visible for the earliest time point. The initial entry rate (k_1) was >10 μm/s, and the intragel diffusion constant ≈0.1 $\mu m^2/s$, corresponding to a passage time of 12 ms through a 50 nm thick hydrogel layer. For computer-simulation, see Figure S5.

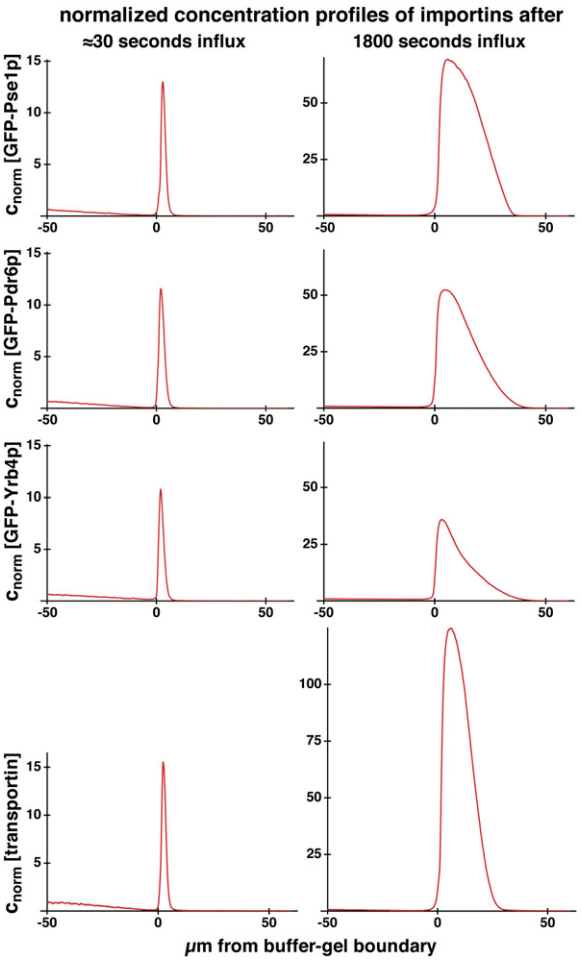

Figure 3. Influx of Other NTRs into the Saturated FG-Hydrogel

A saturated FG-hydrogel was prepared, and influx of indicated NTRs was measured as in Figure 2. Panels give concentration profiles of the diffusing species, normalized to the free concentration in buffer (outside the depletion zones).

concentration profile we estimated that the concentration-normalized entry rate into the FG-hydrogel is at least 1000× higher for importin β than for acRedStar (Table 1; Experimental Procedures).

Crucially, GFP-importin β did not remain stuck at the surface of the hydrogel. Instead, the importin β-ingression zone spread deep into the gel, nearly 50 μm within 30 min (Figures 2 and S3). Even though the diffusion constant of ≈0.1–0.2 $\mu m^2 \cdot s^{-1}$ is ≈200- to 500-fold lower than free in solution, it is still fast enough for traversing the distance through the central NPC channel of vertebrate pores (≈50 nm) in 6–12 ms. This number is remarkably close to passage times of NTF2 (5.8 ms), transportin (7.2 ms), and importin β-cargo complexes (10 ms) through authentic NPCs of cultured mammalian cells (Kubitscheck et al., 2005; Yang et al., 2004).

It should be noted that the FG-hydrogel also showed its NPC-like behavior when probed with other model proteins and permitted rapid, facilitated entry of the yeast importins Pse1p/Kap121p, Pdr6p/Kap122p, Yrb4p/Kap123p, as well as of the human importin transportin 1 (Figure 3; Table 1).

Its sieve-like nature predicts that the FG-hydrogel excludes smaller inert proteins less efficiently. Indeed, the influx of our variant of the green fluorescent protein ("acGFP"; R_S = 2.5 nm) occurred ≈100× faster than influx of acRedStar (R_S = 3.9 nm), but, still, it was ≈500-fold delayed as compared to crossing a water-water boundary

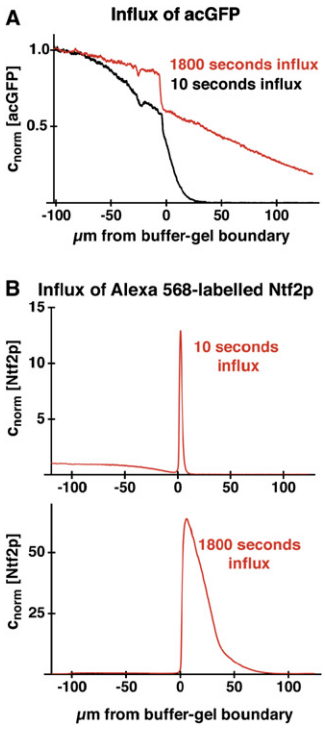

Figure 4. Influx of GFP and Ntf2p into the Saturated FG-Hydrogel

A saturated FG-hydrogel was prepared, and influx of acGFP (A) or fluorescently labeled yeast Ntf2p (B) was measured as in Figures 1–3.

(computed as crossing a 50 nm thick water-layer; Figure 4; Table 1).

Ntf2p has a similar Stokes radius and charge as acGFP and functions as the nuclear import receptor of Ran (Ribbeck et al., 1998). It is therefore capable of facilitated NPC passage. Consistent with that, its entry into the saturated FG-hydrogel occurred at least 20-fold faster than that of acGFP (Figure 4; Table 1). Thus, also for GFP-sized objects, the FG-hydrogel could correctly discriminate between inert molecules and nuclear transport receptors.

Extrapolation to Barrier-Filled Channels

So far we have considered only the entry of our model proteins into the hydrogel and their movement within the gel. The more crucial question is, however, how fast they would cross an NPC-sized hydrogel layer; this includes not only gel entry and intragel movement, but also the exit from the gel. As detailed in Figure S4, the steady-state flux J through a gel-filled channel can be approximated as:

$$J = -\frac{A \cdot D \cdot k_1 \cdot \Delta c}{L \cdot k_{-1} + 2D} \qquad (2)$$

Here, A is the cross-section, L the length of channel, D the intragel diffusion constant, k_1 the entry rate into the barrier, k_{-1} the exit rate, and Δc the nucleo-cytoplasmic concentration difference of the diffusing species.

An interesting implication from Equation 2 is that the selectivity of the barrier, i.e., the quotient between the passage rates of two different species, not only depends on the barrier material, but also on the length of the barrier-filled channel.

Using digitonin-permeabilized HeLa cells as an experimental system, we previously found that NPCs permit a flux of 2 GFP molecules per pore, second, and 1 μM nucleocytoplasmic concentration difference (Ribbeck and Görlich, 2001). Pores filled with the Nsp1-derived saturated FG-hydrogel would make an even better barrier and permit an acGFP-flux of only $\approx 0.3 \frac{molecules}{pore \cdot second \cdot \mu M}$ (see Table 1). The ≈100-fold slower influx of the larger acRedStar protein further supports the assumption that the reconstituted FG-hydrogel performs as a barrier at least as well as authentic NPCs do.

Cargo-free transportin was found to cross authentic NPCs with a rate of 65 $\frac{molecules}{pore \cdot second \cdot \mu M}$ (Ribbeck and Görlich, 2001). For a pore containing the Nsp1-derived saturated FG-hydrogel, we would expect passage rates for transportin and the GFP-tagged yeast importins Pse1p, Yrb4p, Pdr6p, and importin β between >4 and >20 $\frac{molecules}{pore \cdot second \cdot \mu M}$ (Figures 2, 3, and S3; Table 1). Since influx is limited by diffusion to the gel and since the depth of the depletion zone in front of the barrier is probably underestimated, these numbers must be considered only as lower limits. It is therefore well possible that these importins enter the Nsp1-derived fsFG-hydrogel as efficiently as they enter bona fide NPCs.

The FG-Hydrogel Even Reproduces Importin-Mediated Cargo Influx

Even though cargo-free NTRs must traverse NPCs during recycling reactions, their actual task is the transport of cargoes. So far, we mimicked the cargo only by the GFP tag fused to the importins. However, we also wished to test if the signal-mediated recruitment of an importin could speed up the barrier entry of an inert molecule.

For this purpose, we fused the IBB domain, a strong importin β-dependent nuclear import signal (Görlich et al., 1996a; Weis et al., 1996) to the acRedStar protein. As expected, the import signal alone was insufficient to improve gel entry of acRedStar (Figure 5, left).

We then preformed a complex with four molecules of importin β per IBB-RedStar tetramer. This increased the mass of the translocating species from 150 kDa to 530 kDa. Nevertheless, this complex entered the gel ≈25,000-fold faster than IBB-RedStar alone (Figure 5). As already observed for the GFP-importin β fusion, a deep depletion zone formed in front of the barrier, indicating that the process was largely limited by the diffusion to the gel. Intragel diffusion was only a little slower than observed for the GFP-importin β fusion and occurred rapidly enough for crossing an NPC within 12 ms. Thus, the saturated FG-hydrogel could also reproduce importin-mediated entry of a signal-bearing cargo molecule.

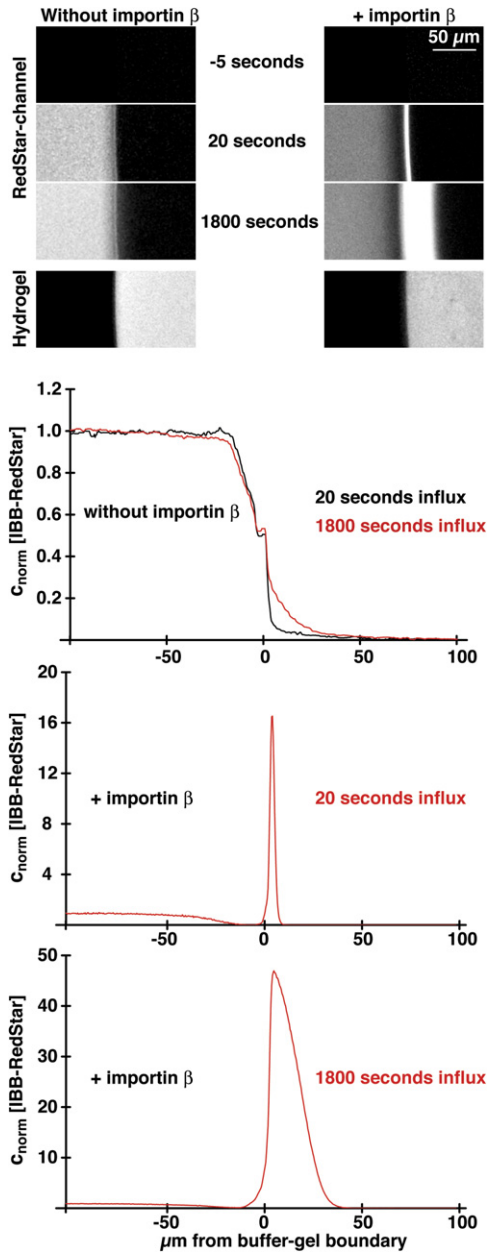

Figure 5. Importin-Mediated Cargo Transport into a Saturated FG-Hydrogel

Preparation of the saturated FG-hydrogel and measurement of gel entry was as in Figures 1–4. As permeation probe, we used a fusion between acRedstar and the IBB domain, a strong nuclear import signal. Prior binding of the cognate nuclear import receptor importin β increased the influx rate of IBB-RedStar ≈25,000-fold. Influx was then limited only by diffusion to the FG-hydrogel. Diagrams show at indicated time points the profiles of IBB-RedStar concentration across the buffer-barrier boundaries. See also Figure S5 for discussion of profile shapes.

The partition coefficient of the importin β-IBB-RedStar complex between buffer and hydrogel was very high (>1000), speaking not only for a high entry rate, but also for a slow exit from the barrier. Since four importin β molecules each contributed to the interaction with the gel, this was not unexpected. It might appear counterintuitive, but a slower exit rate should make barrier-passage more efficient because it suppresses a premature exit on the *cis*-side of the barrier and gives more time for diffusion to the *trans*-side (see Equation 2). A slow exit rate at the *trans*-side can, in the simplest case, be compensated by building up a higher concentration of the mobile species within the barrier (Equation 2). The exit rate from the gel will then no longer limit the steady-state flux.

Too slow an exit rate will, however, increase the residence time at NPCs and eventually even clog NPCs that operate under high transport load. For both problems, it will help that exit from the permeability barrier into the destination compartment is normally actively enforced in vivo—for example, when nuclear RanGTP dissociates importin-cargo complexes (Rexach and Blobel, 1995; Görlich et al., 1996b) and weakens interactions of importin β with nucleoporins from the nuclear side of the NPC (Shah et al., 1998). This should be particularly important if the cargo-NTR complex has a very high partition coefficient. This perfectly agrees with what has been observed for importin β-mediated cargo import into mammalian nuclei, where the efficient completion of NPC passage requires the terminating action of nuclear RanGTP (Görlich et al., 1996b).

DISCUSSION

The permeability barrier can be considered as the "active zone" of NPCs. The barrier itself is a passive and yet extremely efficient sorting device. On the one hand, it suppresses an uncontrolled intermixing of nuclear and cytoplasmic contents. On the other hand, it permits rapid passage of NTRs, and it combines with NTRs and the RanGTPase-system to form a high-capacity cargo pump. Crucially, it must remain a barrier toward inert macromolecules, even when much larger NTR-cargo complexes pass. This suggests that the barrier is made of a highly adaptive material that seals tightly around any translocating species.

We now have such barrier material at hand and can study its fascinating properties in the test tube. It behaves like predicted previously in the selective phase model (Ribbeck and Görlich, 2001): it is an FG-repeat hydrogel that is entered only very slowly by large inert macromolecules, but up to 25,000-fold faster by NTRs and NTR-cargo complexes. Since the passage rate through the barrier is primarily determined by the entry rate (Equation 2), this difference in entry rates can explain macroscopically how the barrier can function as an effective sorting machine. Remarkably, the in vitro-formed FG-hydrogel can even reproduce signal- and importin-mediated cargo influx (Figure 5).

On a molecular level, the barrier is a 3D sieve, whereby meshes form through hydrophobic and/or π-π

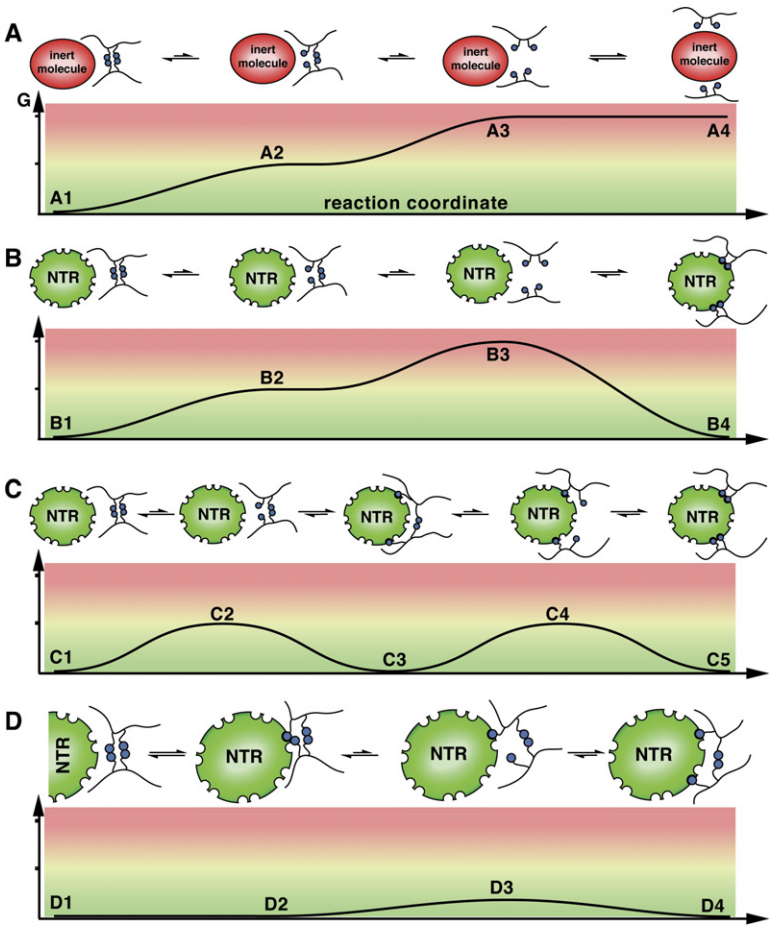

Figure 6. Model for Self-Catalyzed Entry of NTRs into the FG-Hydrogel

(A) Exclusion of inert objects that do not interact with the hydrophobic clusters of FG repeats. An interrepeat contact, comprising two pairs of interacting phenylalanines (blue), obstructs the path of an inert object into the FG-hydrogel. Such an obstacle, however, does not pose an absolute barrier. Instead, thermal motion can bring the interacting phenylalanine side chains to (higher energy) states, where one ("A2") or even both half contacts ("A3") are transiently broken. The energy barrier between "A1" and "A3" suppresses the gel entry of the inert object; the rate of complete contact dissociation sets an upper limit for the gel-entry rate.

(B) Scenario where NTRs can bind a contact site only after its full dissociation. Gel entry is also here limited by the (spontaneous) rate of complete contact dissociation. Such NTR can therefore pass the obstacle not faster than the inert object from scenario A. Thus, NTRs can accelerate interrepeat dissociation only if they stabilize spontaneous dissociation-intermediates (C) and/ or directly destabilize fully closed contacts (D).

(C) Scenario where NTRs can trap phenylalanine side chains already from a half-dissociated contact ("C3"). The released binding energy lowers the energy barrier for reaching the fully dissociated state ("C4"), allowing faster gel entry than in (B). The rate of half-dissociating interrepeat contacts sets an upper limit for the gel-entry rate in this scenario.

(D) Scenario where NTRs can already bind and destabilize a fully closed contact. In combination with scenario C, this would provide the flattest energy landscape and allow the fastest entry into the gel.

interactions between individual repeat units of the FG-repeat domains. The meshes allow free passage of small molecules but restrict barrier entry of inert molecules that exceed the mesh size. It is thought that NTRs overcome this size limit because they bind hydrophobic clusters from disengaged interrepeat contacts and thereby keep an otherwise obstructing interrepeat contact "opened."

The selective phase model made several key predictions that could subsequently be confirmed in this and previous studies (Frey et al., 2006; Ribbeck and Görlich, 2002). Nevertheless, we are still far from fully understanding the mechanism of NPC passage. In particular, the kinetics of gel entry and intragel movement still need to be explained. In the following, we attempt a qualitative explanation.

Refinement of the Selective Phase Model

Large inert molecules as well as NTRs and their cargo complexes exceed the mesh size of the FG-hydrogel. They can therefore enter the gel only when interrepeat contacts disengage (Figure 6). Given the very slow entry of acRedStar into the hydrogel, one should expect a very slow spontaneous dissociation of interrepeat contacts within a saturated FG-hydrogel. GFP-importin β and the importin β-cargo complex entered the gel three to more than four orders of magnitude faster than acRedStar (Figures 1, 2, 5, and S3; Table 1). This would be impossible if NTRs had to "wait" for spontaneous disengagement of interrepeat contacts (Figure 6B). Instead, NTRs must greatly increase the dissociation rate of adjacent interrepeat contacts. To achieve this, it is not sufficient for NTRs to bind the end products of dissociation (Figure 6B). Instead, NTRs must act already on closed interrepeat contacts, destabilize those contacts, and make dissociation intermediates energetically more favorable.

How might this work? Hydrophobic clusters from FxFG repeats contain two hydrophobic residues. The corresponding interrepeat contacts should therefore comprise two hydrophobic or π-π interactions (illustrated in Figure 6). While inert molecules must "wait" for the spontaneous breakage of a complete interrepeat contact before they can pass the obstacle (Figure 6A), NTRs could already trap a phenylalanine side chain from a

half-dissociated contact (Figure 6C). This would stabilize the dissociation intermediate until the second half-contact has also dissociated. This way, NTRs could "catalyze" the dissociation of interrepeat contacts (Kustanovich and Rabin, 2004) by reducing the required activation energy (Figure 6C).

NTRs could even "melt" the contact directly provided they are able to bind to a Phe side chain from a closed interrepeat contact (Figure 6D). Spending the released binding energy on weakening the interaction between the two Phe side chains would then lower the energy barrier for dissociating interrepeat contacts (Figure 6D). The combination of the two just-described mechanisms would provide a very flat energy landscape for interrepeat dissociation and hence allow for a rapid entry of NTRs into the FG-hydrogel. The scenario here has been described for FxFG repeats but should also apply to GLFG repeats that also contain 2 hydrophobic residues per cluster.

NTRs possess multiple binding sites for FG repeats and hence interact multivalently with the FG-hydrogel (Bednenko et al., 2003; Kutay et al., 1997; Morrison et al., 2003). Multivalency increases further when cargoes recruit more than one NTR molecule (as in Figure 5). Such multipoint anchorage should suppress any intra gel movement unless repeat-NTR interactions are very dynamic. To be consistent with the intragel diffusion constants (Table 1), individual repeat-NTR contacts must indeed rearrange at a timescale of 100 μsec or faster (for estimation, see Experimental Procedures). Such rapid kinetics can also be explained by the model outlined above (Figure 6). The model comprises a series of reversible steps and therefore predicts a flat energy landscape not only for the NTR-assisted dissociation of interrepeat contacts, but also for the back reaction. In other words, FG repeats from the gel must accelerate the dissociation of repeat-NTR contacts by the same large factor as NTRs accelerate the dissociation of interrepeat contacts.

Biogenesis of the Permeability Barrier

The permeability barrier anchored within the rigid NPC scaffold is of only nanoscopic scale. For studying the permeability properties of the FG-hydrogel we needed, however, a gel that was homogeneous over ≈100 μm. To prepare such a gel, we started from a homogeneous aqueous solution of the fsFG-repeat domain (adjusted to low pH, where the repulsive, positive net charge of the polymer suppressed self-association) and triggered gelation by adjusting a physiological pH. It is clear that cells cannot use the same trick to assemble NPCs, and this poses the question as to how a hydrogel-based permeability barrier could form in vivo. It is also legitimate to ask whether NPCs contain a sufficient number of FG-repeat units to form a saturated FG-hydrogel.

The transporter region of a yeast NPC appears significantly smaller than its vertebrate counterpart. It has a diameter of 35 nm, a length of 30 nm (Yang et al., 1998), and thus a volume of $\approx 3 \times 10^4$ nm^3. Estimated from the copy number of the individual Nups per NPC (Rout et al., 2000), a single yeast NPC should contain a total of ≈5000 FG-repeat units (8.7×10^{-21} moles). This would be sufficient to fill a volume of 1.7×10^5 nm^3, i.e., 6× the volume of the central channel, with a (saturated) 50 mM FG-hydrogel. Even considering that not all repeat domains contribute to the barrier at the central channel and that half the repeat domains can be deleted without compromising viability (Strawn et al., 2004), it therefore appears that NPCs indeed contain a sufficient number of FG repeats to form a saturated FG-hydrogel within the central channel. In addition, a large proportion of the volume of the central channel is normally occupied by NTRs and cargo in transit. Such displacement will lower the overall FG-repeat concentration required for making a saturated gel inside the central channel.

Since the FG-repeat domains are anchored to the scaffold of the NPC, the NPC-assembly process will force them to a sufficiently high local concentration. One problem, however, remains—namely that the FG-repeat domains need to be arranged inside the central channel such that they do not just fold back on themselves but instead engage into interdomain contacts to form an efficient barrier. We suggest that NTRs are crucial for that. Just as they catalyze the rearrangements necessary for their own barrier passage, they should be able to smooth out nonproductive interactions within the permeability barrier. In addition, they probably associate with newly synthesized FG-repeat Nups and thereby suppress, as molecular chaperones, nonproductive interactions during transit to the NPC-assembly sites. These complexes should be rather stable as long as the local repeat concentration is low. At higher repeat concentrations, interrepeat interactions should become favored, leading to a release of repeat domains from their chaperones into the nascent permeability barrier. It has previously been reported that importin β participates in NPC assembly, both in higher eukaryotes and in yeast (Harel et al., 2003; Ryan et al., 2007; Walther et al., 2003). We would now suggest that this not only ensures that NPCs are built at the right place (within the NE) but also that NTRs act as assembly factors for the permeability barrier.

It is well established that interactions between NTRs and FG-repeat domains are a prerequisite for facilitated NPC passage, and therefore it has been suspected that these domains are part of the barrier (see e.g., Ribbeck and Görlich, 2001; Rout et al., 2000). Our data now demonstrate that such domains can indeed build a highly efficient and selective barrier that excludes normal macromolecules but permits an at least 1000-fold faster passage of NTRs and their cargo complexes. However, an FG-hydrogel is not yet sufficient to form such an efficient barrier. Instead, the local repeat concentration must exceed the saturation limit so that all hydrophobic clusters can engage into pairwise contacts. Such conditions most likely prevail within the central channel. Our data therefore strongly suggest that a saturated hydrogel indeed represents the functional form of the permeability barrier of NPCs.

Evolutionary Implications

NPCs consist of ≈30 different nucleoporins, which raises the question of how such complex structure could have emerged in evolution. It is clear that only a functional version could have provided a competitive advantage. However, it appears impossible that so many proteins evolved exactly at the same time and then already had the compatibility to form one operational unit. For the "active zone" of the NPC, our data might now resolve the problem. They suggest that the transport function per se does not require a complex composition. Instead, primordial NPCs could have been operational with a permeability barrier built from multiple copies of just a single FG-repeat domain.

EXPERIMENTAL PROCEDURES

E.coli Expression Vectors

The backbone of the indicated plasmids was derived from pQE80 (QIAGEN, Hilden, Germany). Plasmids allowed for recombinant expression of indicated proteins in *E.coli*. Plasmids used are listed in Table S1. Their sequences are available on request.

Expression and Purification of Diffusion Substrates and Transport Receptors

Proteins were expressed in *E.coli* and purified on Nickel-Sepharose. Imidazole-eluted fractions were further purified by gel filtration on a Superdex 200 column (Pharmacia) equilibrated with buffer A (50 mM Tris/HCl pH 7.5, 200 mM NaCl, 1 mM EDTA, 2 mM DTT).

In the case of acGFP, the His_{10}-ZZ-tag was cleaved off with TEV protease and removed before gel filtration.

Untagged yeast Ntf2p was purified as human NTF2 (Ribbeck et al., 1998) and labeled with AlexaFluro568-maleimide via an engineered C-terminal cysteine. Alexa488-labeled transportin was described before (Ribbeck and Görlich, 2001).

Expression, Purification, and Labeling of Nsp1 fsFG-Repeat Domain

The N-terminally His_{10}-tagged Nsp1 fsFG-repeat domains were expressed and purified as described (Frey et al., 2006). To obtain fluorescently labeled FG-repeat domains, the C-terminal cysteine was reacted with AlexaFluor633-maleimide. The labeled fsFG-repeat domain was further purified by gel filtration.

Preparation of FG-Repeat Hydrogels

The starting points for gelation were salt- and solvent-free preparations of the fsFG-repeat domain from Nsp1p. For that, the nickel-eluted protein was applied to a reverse-phase HPLC column, eluted with increasing concentration of acetonitrile in 0.1% TFA, and lyophilized. The lyophilized protein was then dissolved at a concentration of 0.34–2.7 mM in 0.1% TFA (in water) containing 1 μM AlexaFluor633-labeled Nsp1 fsFG repeats, followed by quick neutralization with 1/4 volume neutralization buffer (400 mM Tris-base, 100 mM Tris/HCl pH 7.5, 1 M NaCl). Two microliter drops were immediately spotted onto uncoated 18-well μ slides (ibidi, Munich, Germany) and were allowed for 48 hr to complete gelation. Amounts and concentrations of the fsFG domain were estimated gravimetrically (assuming Mr = 64 kDa for the free protein and 74 kDa for the TFA salt).

Others (Patel et al., 2007) reported difficulties in detecting homotypic interactions of the Nsp1-fsFG domain. This probably reflects that fact that interrepeat contacts are designed to be weak, but also technical problems, such as their choice of nonphysiological binding conditions.

Microscopy

FG-hydrogels were equilibrated for at least 90 min in a large excess of buffer A. Gel entry of fluorescent substrate molecules was assayed using an SP5 confocal laser scanning microscope equipped with a 20× or 63× immersion objective (Leica, Bensheim, Germany). Briefly, the buffer-gel boundary was positioned in the center of the observable area, and the focal plane was set to 15 μm above the surface of the slide. One hundred and twenty one frames (2048 × 256 pixels) were recorded in 15 s intervals in appropriate channels, using the 633 nm laser line to monitor the position of the gel and either the 488 nm laser line (for GFP- or Alexa 488-fluorescence) or the 561 nm laser line (for acRedStar- or Alexa 568-fluorescence). Fluorescent substrates (in buffer A) were added after recording of the first frame. acRedStar and IBB-acRedStar were used at 1 μM (tetramer), and transport complexes were preformed from 1 μM IBB-acRedStar tetramer and 4 μM importin β. Other substrates were used at 3 μM.

Analysis of Microscopical Data

All numerical operations had been implemented in Mathematica 5.2. Individual frames were first converted to concentration profiles. To correct for deviations of the buffer-gel boundary from a perfectly perpendicular orientation to the lines of the frames, we first aligned all lines with each other before we averaged all 256 lines to yield the corrected profile. The image of the hydrogel served as reference for the alignment. Such corrected profiles are shown in Figures 1–5 and S3 and were used for all further computations. Before estimating the depths of the depletion zone in front of the gel, profiles were smoothed by an exponential filter.

Estimation for the Rates of Gel Entry

To determine the amount of fluorescent material that had entered the hydrogel at a given time point, the corrected profiles were normalized to the free concentration in buffer (outside the depletion zones) and subsequently numerically integrated. Diffusion within low-concentrated gels was very fast, and the intrusion zone was spread for later time points beyond the imaged area. In these cases, the concentration profiles were extrapolated to a distance of up to 1 mm, and the extrapolated profiles were then used for integration.

Crude influx rates were determined as the change of gel-accumulated protein over time and normalized to the cross-section of the buffer-gel boundary.

NTRs enter the FG-hydrogel against a gradient of absolute concentration. Therefore, the influx can only be described by considering chemical activities:

$$\frac{influx(t)_{across\_boundary}}{Area_{of\_boundary}} = -k_1 \cdot \Delta a(t)_{across\_boundary}, \quad (3)$$

where "k_1" is the normalized entry rate [units m/s], and "*a*" stands here for the chemical activity of the transported species and is related by $a = f \times c$ to the concentration. f is unity in buffer, while $f = \frac{1}{partition\ cofficient}$ applies for species inside the gel. The concentrations of the transported species at each side of the boundary were estimated for each time point from the concentration profiles. From these numbers and the normalized influx rates, the k_1 values were estimated.

Whenever there were uncertainties, e.g., in the partition coefficient or in the depth of the depletion zone, we made conservative estimates to obtain the smallest k_1 value of NTR influx that was still consistent with the data. The numbers for cases of rapid gel entry given in Table 1 should therefore be considered as lower limits.

The exit rate k_{-1} was estimated from: $partition\ coefficient = \frac{k_1}{k_{-1}}$. Here, it is interesting to note that the exit rate of acRedStar from the saturated FG-hydrogel is not faster than exit of importin β (despite the much higher partition coefficient of importin β). Probably, importin β can dissolve obstructing interrepeat contacts also during gel exit, while inert cargoes cannot, which would be in perfect agreement with the extended selective phase model.

Estimation of Intragel Diffusion Constants

The intragel diffusion constants were estimated by fitting concentration profiles inside the gel at given time points t to the integrated solution of the Ficks second law of diffusion: $c(x,t) = \frac{c_0}{2}[1 - \Phi(u)]$, with x being the distance from the boundary, $u = \frac{x}{2\sqrt{D \cdot t}}$, D the intragel diffusion constant, and $\Phi(u)$ being the error function $\Phi(u) = \frac{2}{\sqrt{\pi}} \int_0^u e^{-y^2} dy$. Alternatively, intragel diffusion constants were estimated by comparing parameters with simulations such as those shown in Figure S5.

Computer Simulation of the Kinetics of Gel Entry

The flux was simulated along an axis perpendicular to the plain of the buffer-gel boundary. By that, the 3D-diffusive process could be simplified to a single dimension. The axis was subdivided into 2000 segments of h = 0.5 μm, and the flux between the segments described by a system of 2000 (computer-generated) ordinary differential equations. Using smaller h-values did not alter the results. The system was numerically solved in Mathematica 5.2, running on a 4 × 2.5 GHz PowerPC G5 machine. Such simulations were routinely used to verify and improve the estimates of the kinetic constants. See Figure S5 for results.

Estimation for the Stability of Interrepeat Contacts in the Vicinity of NTRs

The movement of an NTR from one mesh position to the next occurs over a distance of x ≈4 nm (approximately the mesh size). With $\Delta t = \frac{\Delta x^2}{2 \cdot D}$ and D = 0.1 $\mu m^2/s$, it follows that ≈100 μs are required for such a step. Since several repeat-NTR and repeat-repeat contacts rearrange for one step, individual contacts must break and reform at a much shorter timescale.

Estimation of the Unit Length of the fsFG-Repeat Domain

The distance between two adjacent hydrophobic clusters on the linear polymer depends not only on the lengths of the chemical bonds but also on the backbone conformation. FG-repeat domains are intrinsically unfolded and could adopt any conformation that avoids steric clashes and conforms to the Ramachandran map. This predicted a continuum of possible distances (ranging from close to zero to the maximally extended conformation) and necessitated a statistic procedure for estimating the mean distance u. For that, we generated random sets of 10^6 allowed backbone conformations and averaged the corresponding end-to-end distances (procedure kindly implemented by Dr. Torsten Fischer). This yielded for the regular (19 residues long) fsFG repeats from Nsp1p a unit length of u = 4.14 nm. This number is considerably smaller than the distance in fully extended conformation (6.28 nm), reflecting the "entropic contraction" of the polymer.

Supplemental Data

Supplemental Data include five figures and can be found with this article online at http://www.cell.com/cgi/content/full/130/3/512/DC1/.

ACKNOWLEDGMENTS

We thank T. Fischer for computing lengths of FG-repeat units; G. Schlenstedt for plasmids encoding yeast importins; M. Knop for a RedStar2-encoding plasmid; T.A. Rapoport, T. Güttler, V. Cordes, and J.M. Mingot for critical reading of the manuscript; as well as the Deutsche Forschungsgemeinschaft (SFB 638) and the Max-Planck-Gesellschaft for financial support.

Received: January 9, 2007
Revised: March 21, 2007
Accepted: June 13, 2007
Published: August 9, 2007

REFERENCES

Bayliss, R., Ribbeck, K., Akin, D., Kent, H.M., Feldherr, C.M., Görlich, D., and Stewart, M. (1999). Interaction between NTF2 and xFxFG-containing nucleoporins is required to mediate nuclear import of RanGDP. J. Mol. Biol. *293*, 579–593.

Bayliss, R., Littlewood, T., and Stewart, M. (2000). Structural basis for the interaction between FxFG nucleoporin repeats and importin-beta in nuclear trafficking. Cell *102*, 99–108.

Bayliss, R., Leung, S.W., Baker, R.P., Quimby, B.B., Corbett, A.H., and Stewart, M. (2002). Structural basis for the interaction between NTF2 and nucleoporin FxFG repeats. EMBO J. *21*, 2843–2853.

Bednenko, J., Cingolani, G., and Gerace, L. (2003). Importin beta contains a COOH-terminal nucleoporin binding region important for nuclear transport. J. Cell Biol. *162*, 391–401.

Burke, B. (2006). Cell biology. Nuclear pore complex models gel. Science *314*, 766–767.

Chi, N.C., Adam, E.J., and Adam, S.A. (1995). Sequence and characterization of cytoplasmic nuclear protein import factor p97. J. Cell Biol. *130*, 265–274.

Cronshaw, J.M., Krutchinsky, A.N., Zhang, W., Chait, B.T., and Matunis, M.J. (2002). Proteomic analysis of the mammalian nuclear pore complex. J. Cell Biol. *158*, 915–927.

Cushman, I., Palzkill, T., and Moore, M.S. (2006). Using peptide arrays to define nuclear carrier binding sites on nucleoporins. Methods *39*, 329–341.

Denning, D.P., Patel, S.S., Uversky, V., Fink, A.L., and Rexach, M. (2003). Disorder in the nuclear pore complex: the FG repeat regions of nucleoporins are natively unfolded. Proc. Natl. Acad. Sci. USA *100*, 2450–2455.

Denning, D.P., and Rexach, M.F. (2006). Rapid evolution exposes the boundaries of domain structure and function in natively unfolded FG nucleoporins. Mol. Cell Proteomics *6*, 272–282.

Elbaum, M. (2006). Materials science. Polymers in the pore. Science *314*, 766–767.

Enenkel, C., Blobel, G., and Rexach, M. (1995). Identification of a yeast karyopherin heterodimer that targets import substrate to mammalian nuclear pore complexes. J. Biol. Chem. *270*, 16499–16502.

Frey, S., Richter, R.P., and Görlich, D. (2006). FG-rich repeats of nuclear pore proteins form a three-dimensional meshwork with hydrogel-like properties. Science *314*, 815–817.

Fribourg, S., Braun, I.C., Izaurralde, E., and Conti, E. (2001). Structural Basis for the Recognition of a Nucleoporin FG Repeat by the NTF2-like Domain of the TAP/p15 mRNA Nuclear Export Factor. Mol. Cell *8*, 645–656.

Görlich, D., and Kutay, U. (1999). Transport between the cell nucleus and the cytoplasm. Annu. Rev. Cell Dev. Biol. *15*, 607–660.

Görlich, D., Kostka, S., Kraft, R., Dingwall, C., Laskey, R.A., Hartmann, E., and Prehn, S. (1995). Two different subunits of importin cooperate to recognize nuclear localization signals and bind them to the nuclear envelope. Curr. Biol. *5*, 383–392.

Görlich, D., Henklein, P., Laskey, R.A., and Hartmann, E. (1996a). A 41 amino acid motif in importin alpha confers binding to importin beta and hence transit into the nucleus. EMBO J. *15*, 1810–1817.

Görlich, D., Pante, N., Kutay, U., Aebi, U., and Bischoff, F.R. (1996b). Identification of different roles for RanGDP and RanGTP in nuclear protein import. EMBO J. *15*, 5584–5594.

Harel, A., Chan, R.C., Lachish-Zalait, A., Zimmerman, E., Elbaum, M., and Forbes, D.J. (2003). Importin beta negatively regulates nuclear membrane fusion and nuclear pore complex assembly. Mol. Biol. Cell *14*, 4387–4396.

Hurt, E.C. (1988). A novel nucleoskeletal-like protein located at the nuclear periphery is required for the life cycle of Saccharomyces cerevisiae. EMBO J. *7*, 4323–4334.

Iovine, M.K., Watkins, J.L., and Wente, S.R. (1995). The GLFG repetitive region of the nucleoporin Nup116p interacts with Kap95p, an essential yeast nuclear import factor. J. Cell Biol. *131*, 1699–1713.

Kubitscheck, U., Grunwald, D., Hoekstra, A., Rohleder, D., Kues, T., Siebrasse, J.P., and Peters, R. (2005). Nuclear transport of single molecules: dwell times at the nuclear pore complex. J. Cell Biol. *168*, 233–243.

Kustanovich, T., and Rabin, Y. (2004). Metastable network model of protein transport through nuclear pores. Biophys. J. *86*, 2008–2016.

Kutay, U., Izaurralde, E., Bischoff, F.R., Mattaj, I.W., and Görlich, D. (1997). Dominant-negative mutants of importin-beta block multiple pathways of import and export through the nuclear pore complex. EMBO J. *16*, 1153–1163.

Morrison, J., Yang, J.C., Stewart, M., and Neuhaus, D. (2003). Solution NMR study of the interaction between NTF2 and nucleoporin FxFG repeats. J. Mol. Biol. *333*, 587–603.

Patel, S.S., Belmont, B.J., Sante, J.M., and Rexach, M.F. (2007). Natively unfolded nucleoporins gate protein diffusion across the nuclear pore complex. Cell *129*, 83–96.

Pemberton, L.F., and Paschal, B.M. (2005). Mechanisms of receptor-mediated nuclear import and nuclear export. Traffic *6*, 187–198.

Rexach, M., and Blobel, G. (1995). Protein import into nuclei: association and dissociation reactions involving transport substrate, transport factors, and nucleoporins. Cell *83*, 683–692.

Ribbeck, K., and Görlich, D. (2001). Kinetic analysis of translocation through nuclear pore complexes. EMBO J. *20*, 1320–1330.

Ribbeck, K., and Görlich, D. (2002). The permeability barrier of nuclear pore complexes appears to operate via hydrophobic exclusion. EMBO J. *21*, 2664–2671.

Ribbeck, K., Lipowsky, G., Kent, H.M., Stewart, M., and Görlich, D. (1998). NTF2 mediates nuclear import of Ran. EMBO J. *17*, 6587–6598.

Rout, M.P., and Wente, S.R. (1994). Pores for thought: nuclear pore complex proteins. Trends Cell Biol. *4*, 357–364.

Rout, M.P., Aitchison, J.D., Suprapto, A., Hjertaas, K., Zhao, Y., and Chait, B.T. (2000). The yeast nuclear pore complex: composition, architecture, and transport mechanism. J. Cell Biol. *148*, 635–651.

Ryan, K.J., Zhou, Y., and Wente, S.R. (2007). The karyopherin kap95 regulates nuclear pore complex assembly into intact nuclear envelopes in vivo. Mol. Biol. Cell *18*, 886–898.

Shah, S., Tugendreich, S., and Forbes, D. (1998). Major binding sites for the nuclear import receptor are the internal nucleoporin Nup153 and the adjacent nuclear filament protein Tpr. J. Cell Biol. *141*, 31–49.

Strawn, L.A., Shen, T., Shulga, N., Goldfarb, D.S., and Wente, S.R. (2004). Minimal nuclear pore complexes define FG repeat domains essential for transport. Nat. Cell Biol. *6*, 197–206.

Suntharalingam, M., and Wente, S.R. (2003). Peering through the pore: nuclear pore complex structure, assembly, and function. Dev. Cell *4*, 775–789.

Walther, T.C., Askjaer, P., Gentzel, M., Habermann, A., Griffiths, G., Wilm, M., Mattaj, I.W., and Hetzer, M. (2003). RanGTP mediates nuclear pore complex assembly. Nature *424*, 689–694.

Weis, K. (2002). Nucleocytoplasmic transport: cargo trafficking across the border. Curr. Opin. Cell Biol. *14*, 328–335.

Weis, K., Ryder, U., and Lamond, A.I. (1996). The conserved amino-terminal domain of hSRP1 alpha is essential for nuclear protein import. EMBO J. *15*, 1818–1825.

Yang, Q., Rout, M.P., and Akey, C.W. (1998). Three-dimensional architecture of the isolated yeast nuclear pore complex: functional and evolutionary implications. Mol. Cell *1*, 223–234.

Yang, W., Gelles, J., and Musser, S.M. (2004). Imaging of single-molecule translocation through nuclear pore complexes. Proc. Natl. Acad. Sci. USA *101*, 12887–12892.